Birte Größner-Schreiber
Maren Herzog
Jürgen Hedderich
Alexander Dück
Matthias Hannig
Michael Griepentrog

Focal adhesion contact formation by fibroblasts cultured on surface-modified dental implants: an *in vitro* study

Authors' affiliations:
Birte Größner-Schreiber, Maren Herzog, Clinic of Restorative Dentistry and Periodontology, University of Kiel, Kiel, Germany
Jürgen Hedderich, Department of Medical Informatics and Statistics, University of Kiel, Kiel, Germany
Alexander Dück, Michael Griepentrog, BAM Federal Institute for Materials Research and Testing, Berlin, Germany
Matthias Hannig, Clinic of Operative Dentistry, Periodontology and Preventive Dentistry, Saarland University, Homburg, Germany

Correspondence to:
Dr Birte Größner-Schreiber
Clinic of Restorative Dentistry and Periodontology
University of Kiel
Arnold-Heller-Str. 16
D-24105 Kiel
Germany
Tel.: +49 0 431 597 2796
Fax: +49 0 431 597 2950
e-mail: groessner-schreiber@konspar.uni-kiel.de

Date:
Accepted 30 January 2006

To cite this article:
Größner-Schreiber B, Herzog M, Hedderich J, Dück A, Hannig M, Griepentrog M. Focal adhesion contact formation by fibroblasts cultured on surface modified dental implants: an *in vitro* study.
Clin. Oral Impl. Res. **17**, 2006; 736–745
doi: 10.1111/j.1600-0501.2006.01277.x

Key words: fibroblasts, focal adhesion contacts, immunogold labeling, hard coatings, titanium implants

Abstract: A major consideration in designing dental implants is to create a surface that provides strong attachment of the implant to bone, connective tissue and epithelium. The aim of the present study was to examine the influence of different treatments of titanium (Ti) implant surfaces on focal adhesion contact (FAC) formation in fibroblast cultures. Human gingival fibroblasts were cultured on glass sheets and polished Ti discs with different surface coatings (applied by physical vapor deposition (PVD): Ti, titanium nitride (TiN), zirconium nitride (ZrN)) or on Ti discs with different surface topographies. For characterization of all surfaces, modified estimation of surface roughness and spacing parameter was carried out using a contact stylus profilometer. Contact angle measurements were carried out to calculate surface energy. Fibroblasts were prepared for transmission electron microscopy at day 3 after seeding, and the number of FACs and the ratio FAC/cellular cross-sections was determined at a length of 300 μm in ultrathin sections. To visualize the extracellular fibronectin and vitronectin molecules and the intracellular actin and vinculin in FAC areas, immunogold labeling was performed. The results revealed a strong correlation between the number of FACs and the surface roughness. The highest number of FACs and the majority of the immunogold-labeled intra- and extracellular matrix molecules were counted on surfaces with the lowest surface roughness: glass sheets coated with either Ti, TiN or ZrN (roughness average = 0.03–0.1 μm). These surfaces appear to favor cellular attachment of human gingival fibroblasts and moreover in previous studies the hard coatings have been shown to reduce bacterial adhesion.

The long-term success of a dental implant strongly depends on good adhesion of the surrounding tissue to the biomaterial. Attachment of the gingiva to dental implants and to natural teeth is mediated by the so-called junctional epithelium (JE). The cells of the JE attach to the tooth surface by means of hemidesmosomes, which are specialized adhesion devices (Schwarz et al. 1990). In culture, most cells adhere to their underlying substrate by means of focal adhesion contacts (FACs), which are restricted areas of extremely close contact between the basal cell membrane and the substratum (Burridge et al. 1988; Burridge & Fath 1989; Burridge & Chrzanowska-Wodnicka 1996). Focal contacts can be identified by the presence of the actin binding protein vinculin. They provide sites of mechanical attachment to the extracellular matrix (ECM), and are points at which adhesion-associated signal transduction is initiated. The expression and organization of focal contacts and hemidesmosomes are a reflection and indicator of the efficiency of cell adhesion (Lodish et al.

1995). In addition, cellular behavior such as adhesion, morphologic change, functional alteration and proliferation are greatly influenced by surface properties, including hydrophilicity, roughness, texture and morphology. In extensive investigations of soft tissue responses to oral implant surfaces, it has been shown that surface treatment of implant materials significantly influences the attachment of oral fibroblasts as well as epithelial cells (Pitaru et al. 1984; Inoue et al. 1987; Brunette 1988; Hormia et al. 1991; Könönen et al. 1992; Mustafa et al. 1998).

Besides good connective tissue adhesion in the transmucosal part of an implant, titanium (Ti) implants exposed to the oral cavity require surface modification to inhibit the adherence of oral bacteria (Yoshinari et al. 2000). Parameters like surface roughness and chemical composition of the implant surface were found to have a significant impact on plaque formation. While a rough transmucosal part of an implant will enhance plaque formation, the bony and connective tissue interface requires a porous or microtextured surface to promote tissue ingrowth. From a clinical study on Ti abutments, it was concluded that a certain threshold roughness (around an roughness average (R_a) of 0.2 μm) might be most suitable to obtain a stable soft tissue sealing around transmucosal abutments (Quirynen et al. 1993, 1996; Bollen et al. 1996). A Ti surface that is too smooth, therefore, will prevent cell attachment. However, an increase of surface roughness of the transmucosal portion above the R_a value of 0.2 μm will facilitate early plaque formation. A smoothening below a threshold R_a of 0.2 μm showed no further significant changes, either in the total amount or in the periodontal pathogenicity of adhering bacteria. Therefore, an ideal transmucosal implant surface should not only minimize bacterial adhesion, but at the same time allow epithelial and connective tissue attachment.

Previous *in vitro* and *in vivo* studies have shown that Ti implant surfaces coated with titanium nitride (TiN) or zirconium nitride (ZrN) reduce bacterial colonization compared with other clinically used implant surfaces (Grössner-Schreiber et al. 2001, 2004; Scarano et al. 2003, 2004). The use of an appropriate coating technique allows universal control of the required surface properties, resulting in reproducibly thin and extremely wear-resistant hard coatings on almost any part of an implant (Milosev & Navinsek 1994; Okumiya & Griepentrog 1999).

In summary, it appears that an improvement of the transmucosal part of an implant is still necessary. The aim of the present study was to analyze the influence of different treatments of Ti implant surfaces on FAC formation and the expression of four specific adhesion-related molecules in human gingival fibroblast cultures. Surface preparations (wet grinding, blasting with either glass beads or ceramic beads of different diameters) with R_a- values between 0.03 and 2.2 μm were used and compared against Ti surfaces modified with different physical vapor deposition (PVD) coatings. Special attention was focused onto the Ti and TiN/ZrN coatings to determine whether these antimicrobial surface treatments are as good as or better than other clinically used implant surfaces for supporting fibroblast adhesion.

Material and methods

Preparation of different surface modifications

Seventeen different surface modifications were selected. Based on antimicrobial properties, TiN or ZrN PVD coatings (Grössner-Schreiber et al. 2001) either on glass sheets or on polished Ti discs were compared with uncoated polished Ti and Ti surfaces with different surface roughness between $R_a = 0.03$ and 2.20 μm.

Commercially pure Ti discs (grade 2, Friadent GmbH, Mannheim, Germany) measuring 10 mm in diameter and 4 mm in thickness, and glass sheets (1 mm in thickness and between 0.7 and 0.9 mm^2 in surface area) were used as substrates. Before all surface modifications, the Ti discs were wet ground on silicium carbide (SiC) paper. After mirror-like polishing with Al_2O_3, further surface treatments were performed.

(A) Glass sheets were coated with pure Ti, TiN or ZrN by PVD coating (Ti-glass, TiN-glass, ZrN-glass). (B) Mirror-like polished Ti discs were either coated with Ti (TiN pol) or ZrN (ZrN pol) using PVD coating. PVD coating, performed in the Federal Institute for Materials Research and Testing, BAM (Berlin, Germany), was carried out in an HTC 625 Multilab ABS™ coating system (Hauzer Techno Coating, Venlo, the Netherlands) with unbalanced magnetron sputtering as described previously (Grössner-Schreiber et al. 2001). The thickness of the coatings was about 2.4 μm for Ti, about 1.8 μm for TiN and 2.2 μm for ZrN for all investigated samples. (C) Mirror-like polished Ti discs (Ti-pol) served as controls. (D) To receive different surface topographies on Ti discs wet grinding on SiC paper with different grits was performed (Ti 180, Ti 800, Ti 1200 and Ti 2400). (E) Aligned wet grinding on SiC paper: Ti discs were not allowed to rotate on the paper so that the resulting surface topography shows an anisotropy (Ti 320 aligned). (F) Ti discs were blasted with ceramic (Al_2O_3) beads of different sizes (TiB 125 and TiB 40). (G) Ti discs were blasted with glass beads of different sizes (Ti GSP1, Ti GSP2 and Ti GSP8). (H) Ti discs were coated with an organic–inorganic nanocomposite material of low surface free energy (Leibniz Institute for New Materials, INM, Saarbrücken, Germany). This surface coating was applied by a sol–gel process because of polycondensation of organic-alcoxysilanes, perfluoro-alcoxysilan and metal oxides at a temperature of 230°C. This procedure results in a surface-free energy of 18–20 mJ/m^2. An overview of all prepared surface modifications is given in Table 1.

After surface modification in the Federal Institute for Materials Research and Testing, all modified substrates were only touched with special gloves or sterile forceps to retain contamination as low as possible. Therefore, no special method of sterilization was used to keep parameters that might change surface characteristics of the substrates as low as possible (e.g., Kilpadi & Lemons 1994). The discs were cleaned by ultrasonication in distilled water for 15 min, followed by several rinses with sterile distilled water and a final rinse in acetone. Ti discs or glass sheets were air-dried under a laminar flow hood and then placed on the bottom of Nunc multiwell dishes (24-well plates) until the beginning of experiments.

Characterization of surface topography

A two-dimensional contact stylus profilometer (Perthometer S6P, Perthen, Germany) was used for measuring height (surface roughness) and spacing parameters

Table 1. **Description of the surface topography using a 2D contact stylus profilometer (mean values of R_a and R_z and standard deviations S_{R_a} and S_{R_z} in micrometer for $n = 10$ titanium discs)**

	Surface modification	$R_a \pm S_{R_a}$ (μm)	$R_z \pm S_{R_a}$ (μm)
Ti-glass	Ti PVD coating on glass	0.09 ± 0.02	0.67 ± 0.31
TiN-glass	TiN PVD coating on glass	0.03 ± 0	0.31 ± 0.1
ZrN-glass	ZrN PVD coating on glass	0.03 ± 0	0.31 ± 0.06
	Wet ground (SiC-paper) Ti surface:		
Ti 180	P180: mean grit size 82 μm	0.23 ± 0.02	1.82 ± 0.2
Ti 320 aligned	P320 mean grit size (46.2 ± 1.5 μm)	0.19 ± 0.03	1.34 ± 0.16
Ti 800	P800: mean grit size (21.8 ± 1 μm)	0.19 ± 0.01	1.64 ± 0.12
Ti 1200	P1200: mean grit size (15.3 ± 1 μm)	0.21 ± 0.01	1.36 ± 0.06
Ti 2400	P2400: mean grit size (8.4 ± 0.5 μm)	0.14 ± 0.01	0.99 ± 0.1
Ti pol	Mirror-like polished (OP-S* Al_2O_3) Ti surface Mean grit size 0.2–0.3 μm	0.10 ± 0.01	0.79 ± 0.08
TiN pol	TiN PVD coating on mirror-like polished Ti surface	0.06 ± 0	0.47 ± 0.13
ZrN pol	ZrN PVD coating on mirror-like polished Ti surface	0.05 ± 0	0.65 ± 0.15
	Al_2O_3-blasted pure Ti surface:		
Ti B 40	Grain size 250–425 μm	1.78 ± 0.13	11.50 ± 0.99
Ti B 125	Grain size 0–125 μm	0.92 ± 0.07	6.23 ± 0.63
	Glass (SiO_2)-blasted pure Ti surface:		
Ti GSP 1	Grain size 0–50 μm	0.52 ± 0.06	3.87 ± 0.55
Ti GSP 2	Grain size 40–80 μm	0.61 ± 0.06	4.08 ± 0.68
Ti GSP 8	Grain size 600–800 μm	2.20 ± 0.26	11.65 ± 2.44
Nano	Organic polymer coating, thermal hardening at 230°C	0.38 ± 0.03	2.45 ± 0.14

PVD, Physical vapour deposition.

(mean spacing of profile irregularities) in accordance with DIN EN ISO 4287. To determine surface roughness for every surface modification, five single measurements with a measuring length of 5.6 mm using a cut of 0.8 mm were performed on at least 10 samples. Using these data, the R_a and the mean roughness depth (R_z) were calculated. To calculate the mean spacing of profile irregularities (average spacing RS_m), five measurements on a distance of 100 μm were carried out (RS_m is the average spacing between peaks at the mean line over the evaluation length. A peak is the highest point between an upward and downward crossing of the mean line. It is calculated as the quotient of all peak spacing results and the number of spaces).

Surface wettability

To characterize surface wettability, contact angle analysis was performed on all surface modifications. The tests were performed at least 21 days after preparation. It was assumed that changes in surface wettability after this time period would not be significant. The sessile drop method was used for contact angle measurements with a commercial contact angle meter (G 402, FA. Krüss, Germany). For every surface modification, three measurements (each with at least five drops of distilled water) were made at room temperature to provide adequate replications for statistical analysis. For each drop, contact angle measurements were repeated 25 times.

Cell culture

Fibroblasts were obtained from outgrowth cultures of healthy human gingival tissues excised during extraction of wisdom teeth. After several washes in phosphate-buffered saline (PBS), tissues were minced into small pieces (less than 0.5 mm^2). These pieces of gingival tissues were transferred into 25 cm^2 tissue culture flasks and were allowed to adhere to the bottom for 30 min. Subsequently, 5 ml of Alpha Minimal Essential Medium (MEM, Biochrom, Berlin, Germany) containing 10% fetal bovine serum and antibiotics (100 U/ml medium of penicillin, 100 μg/ml streptomycin) was added. Cultures were maintained at 37°C in humidified air and 5% CO_2. When substantial fibroblast outgrowth had occurred (usually about 3–4 weeks), the cells were released with trypsin and were grown and passaged under standard conditions in 5 ml tissue culture flasks. Cells of the fourth passage were used for the experiments.

Calculation of cell number

Preliminary experiments with fibroblasts cultured on polished Ti discs at different time periods (3, 24, 48 h, 3, 4, 6 and 7 days) were carried out to determine both the best cell passage number to use and plating time. The growth curve revealed an exponential growth of the fibroblasts between day 3 and day 6 after plating, and the growth plateau was reached at day 7. Based on these results, day 3 with cells close to confluence was chosen to carry out the experiments.

Cellular morphology scanning electron microscopy (SEM)

At day 3, cells were rinsed three times with PBS and then fixed with 3% paraformaldehyde for 10 min. After extensive rinsing in PBS, dehydration through a graded series of ethanol from 30%, 50%, 70%, 90% and 100% followed. After air-drying, surfaces were thinly sputter-coated with gold (SCD 030, Balzers Union, Liechtenstein) and examined by SEM (Philips, Eindhoven, the Netherlands). Fibroblasts on polished Ti discs were used as controls. Photographs of discs with different surfaces were obtained both before and following incubation with the fibroblasts.

Processing of fibroblasts for transmission electron microscopy (TEM)

Cells were seeded at a density of 2×10^4 cells/ml onto modified Ti discs. All subsequent experiments were carried out in duplicate. After 3 days of culture, cells were rinsed three times with PBS and then fixed. Fixation was performed with 0.1% glutaraldehyde + 4% paraformaldehyde in PBS for 2 h, followed by dehydra-

tion through a graded series of ethanol from 50%, 70%, 80%, 90% and 100%.

Embedding took place in LR White resin after infiltration with three changes of the resin, and polymerization was carried out in an oven at 60°C for 48 h. After polymerization, Ti discs and glass sheets were dissolved with 5% hydrofluoric acid. The resin blocks were then reembedded in LR White resin to perform ultrathin sectioning. Ultrathin sections (50 nm) were cut, and every fourth cut of each sample (altogether four sections – one section for each antibody) was collected on nickel grids (hexagonal, Plano GmbH, Wetzlar, Germany). Ultrathin sections were used for both the immunogold labeling and the morphometric analysis.

Immunogold-labeling method

To visualize the extracellular fibronectin and vitronectin molecules and the intracellular actin and vinculin in FAC areas, immunogold labeling was performed. Sections on grids were first incubated in ammoniumchloride for 5 min, followed by two rinses in PBS and then blocked with 2% bovine serum albumin (BSA) for 10 min. Sections were then incubated overnight (16–18 h) at 4°C with primary antibodies diluted in PBS (three parts) containing 2% BSA (one part); rabbit anti-vitronectin diluted 1 : 800; sheep anti-fibronectin diluted 1 : 1500; mouse anti-vinculin diluted 1 : 70; and mouse anti-actin diluted 1 : 600 (all primary antibodies: Biotrend, Köln, Germany). Then, the grids were washed (five changes, 5 min each) and bound primary antibodies were visualized by incubating the sections for 2 h with secondary antibodies at room temperature: goat anti-rabbit gold conjugate (10 nm, Biotrend) diluted 1 : 800; rabbit anti-sheep gold conjugate (10 nm, Biotrend) diluted 1 : 1500; and goat anti-mouse gold conjugate (10 nm, Biotrend) diluted 1 : 70 (vinculin), respectively 1 : 600 (actin) in PBS (three parts) containing 2% BSA (one part). Finally, grids were washed on drops of water (three changes, 5 min each) before being fixed in 1% glutaraldehyde (1 min) and washed three times in distilled water. For contrast enhancement, sections were counterstained with 2% aqueous uranylacetate (Servas, Heidelberg, Germany), followed by three rinses in destilled water. Immuno-labeled grids were examined in a TEM (Philips 201 TEM). Fibroblasts on polished Ti discs were used as controls.

Morphometric analysis

All morphometric analysis was performed using prints (Ilford Ilfospeed RC; Kodak electron microscope film) that were taken from ultrathin sections. The number of FACs and the ratio of the number of FACs to the number of cellular cross-sections (FACs/CCSs) in fibroblasts were determined in each ultrathin section on a length of 300 μm. For this purpose, five adjacent hexagons (each about 60 μm in diameter) of the nickel grids that were used for mounting the ultrathin sections needed to be evaluated.

To visualize and count immunogold particles in adhesion-related molecules, four ultrathin sections (one for each antibody) for all of the 17 different surface modifications were examined in the TEM. The analysis (determination of the number of FACs containing adhesion molecules labeled with gold particles on a length of 300 μm) was carried out in duplicate (two Ti or glass discs of each surface modification). Because of the small sample size ($n = 2$ for each antibody), the results of the immunogold labeling were represented by descriptive analysis.

Statistical analysis

All different surface modifications ($n = 17$) were examined in duplicate. Therefore, the number of FACs and the ratio of FACs/CCSs were measured in four sections (one section for each antibody) for each sample (four different antibodies and two samples of each surface: $n = 8$ sections for morphometric analysis). The resulting values were very homogeneous within each surface and could be described by means and standard deviations. Although the variances slightly

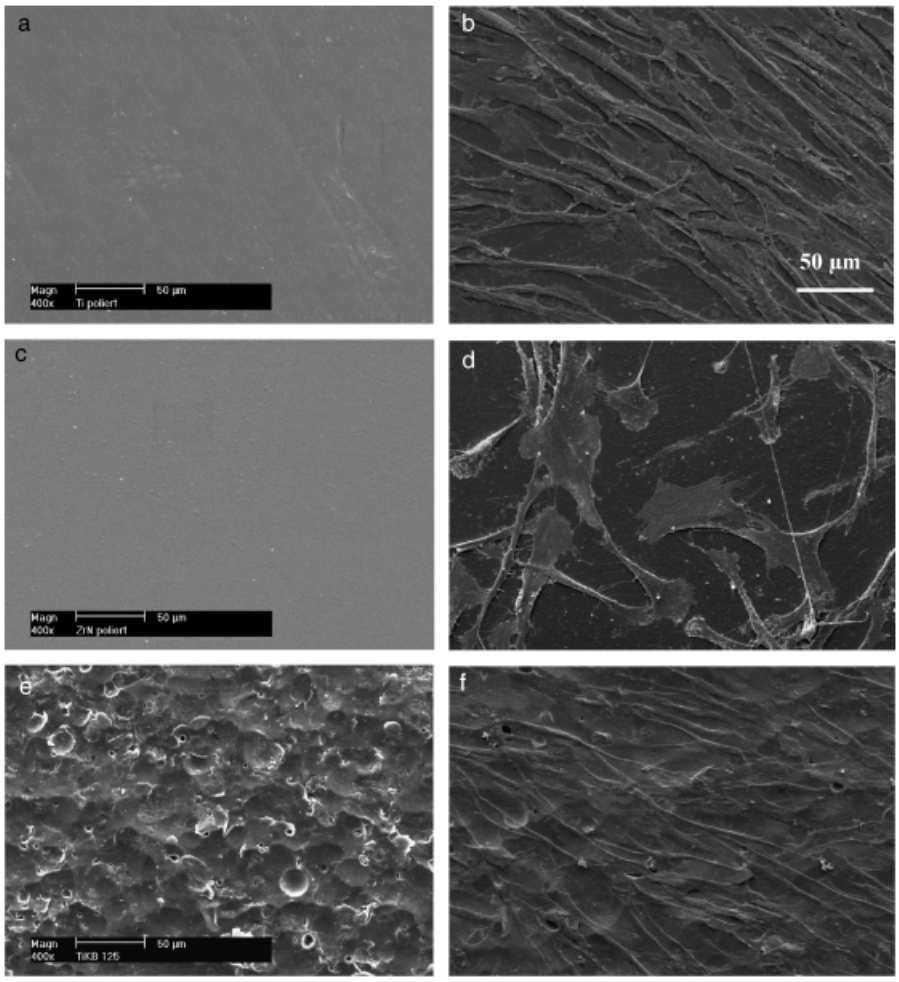

Fig. 1. Scanning electron micrographs of surface-modified titanium (Ti) discs with and without fibroblasts: (a, b) polished Ti, (c, d) zirconium nitride-coated polished Ti, (e, f) Ti disc modified by blasting with ceramic (Al_2O_3) beads (Ti B 125; grain size 0–125 μm). Magnification: a, c, e × 400; b, d, f × 297.

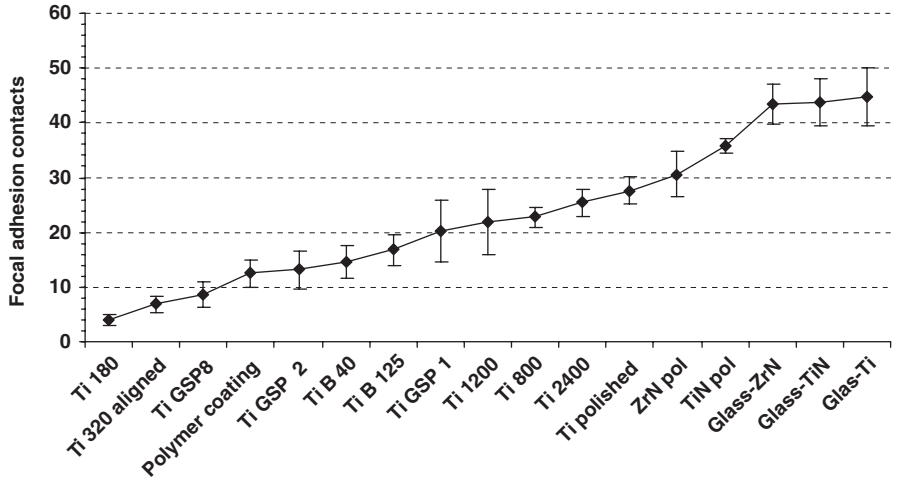

Fig. 2. Number of focal adhesion contacts on a distance of 300 μm (transmission electron microscopy). The horizontal bars indicate homogeneous subgroups based on the Scheffé multiple comparison procedure.

differed between surfaces, differences were analyzed with an analysis of variance (ANOVA), especially by defining homogeneous subgroups based on a multiple comparison procedure (Scheffé) with a level of significance set at 0.05 (Figs 1 and 2). All analyses were performed using SPSS software for Windows.

Results

Characterization of surface topography

The results for surface roughness measurements evaluated with a 2D contact stylus profilometer are shown in Table 1. R_a values varied between 0.03 and 2.2 μm. Surface roughness was not altered by sputtering of a polished Ti surface with nitride. Depending on the method of surface treatment, results of the spacing parameter measurements could be divided in to three groups (results are not shown). Smooth surfaces with R_a values between 0.03 and 0.1 μm (glass surfaces coated with Ti, TiN, or ZrN and uncoated polished Ti or polished Ti coated with TiN or ZrN) showed low RS_{ms} (between 2.3 and 8.3 μm). All surfaces that were wet ground and some of the surfaces that were blasted either with ceramic or glass beads (R_a between 0.14 and 0.92 μm) revealed values between 31 and 64 μm. The highest RS_m was calculated for surface modifications with the roughest surface topography (Ti B 40: R_a 1.78 μm, RS_m 112 ± 40; GSP 8: R_a 2.2 μm, RS_m 146 ± 52 μm).

***Table 2.* Surface wettability measurements of differently modified titanium discs or glass sheets**

Surface	Mean contact angle for water (°)
ZrN glass	109.1 ± 1.7
TiN glass	105.3 ± 4.4
Ti glass	95.6 ± 1.8
ZrN pol	71.3 ± 2.2
TiN pol	73.2 ± 1.5
Ti pol	73.2 ± 1.1
Ti GSP8	45.1 ± 2.8
Ti GSP 1	36.2 ± 2.2
Ti B125	49.3 ± 2.9

Surface wettability

For surfaces modified by wet grinding, the organic–inorganic nanocomposite-coated surface and TiB 40, values of contact angle measurements were not reproducible because of the anisotropy of the different surface topographies. The shape of the drops was highly asymmetric and not stable during the measuring period. Table 2 shows the water contact angles for all other surface modifications. It was found that the water contact angle was strongly dependent on surface morphology. With increasing R_a (from 0.03 to 0.52 μm), the contact angle changed from 109° to 36°. The roughness enhances the wettability of the surface modifications under investigation from a hydrophobic (contact angle $>90°$) to a hydrophilic character (contact angle $<90°$). The lowest contact angle was measured on Ti surfaces modified with glass beads, followed by ceramic bead modification. Polished Ti and polished but cleaned (acetone, ultra sonic bath) Ti surfaces showed similar values (62.6° and 61.3°, respectively). However, the use of different cleaning agents like propanol or ethanol resulted in higher values. Therefore, cleaning with acetone in an ultrasonic bath was used for all Ti and glass surfaces in this study. Compared with a polished Ti surface, PVD coating of a polished Ti surface resulted in slightly higher contact angle values, but glass sheets coated with either Ti, TiN, or ZrN showed distinctly higher values.

Cellular morphology (SEM)

SEM examination revealed that human gingival fibroblasts displayed good adhesion and spread well on all modified surfaces (Fig. 1a–f). However, cellular morphology varied. Fibroblasts cultured on surfaces with an R_a between 0.03 and 0.2 μm (e.g., Ti-glass, ZrN/TiN-glass, Ti-pol, Ti 2400) were mainly spindle shaped and elongated, with no clear orientation (Fig. 1a and b). Cells on Ti 800 and Ti 1200 showed a similar picture and were slightly aligned along grooves produced by the grinding process. Polished Ti discs modified by PVD coating (TiN pol, ZrN pol) showed fibroblasts that were well spread and had a polygonal cell shape. Many cells had a flat morphology and appeared intimately adherent to the surface with many short and strong processes (Fig. 1c and d). On surfaces modified either by organic polymer coating or by blasting with glass or ceramic beads ($R_a = 0.52$–2.2 μm), fibroblasts appeared spindle shaped and did not bridge grooves but formed focal adhesions to the side and bottom of even quite fine grooves or pits (Fig. 1e and f).

Morphometric analysis

Examination of fibroblasts by TEM showed that all cells adhered well and followed the microarchitecture of the underlying substrate surface. The number of FACs (observed on a length of 300 μm) was significantly different between modified surfaces. The means of the number of FACs were divided into eight homogeneous subgroups based on a multiple comparison procedure (Scheffé; Fig. 2). Three subgroups were significantly different from each other: subgroup 1 with Ti 180, Ti 320 aligned, Ti GSP8, polymer coating, Ti GSP2, Ti B 40 and Ti B 125, subgroup 5 with Ti GSP, Ti 1200, Ti 800, Ti 2400, Ti

polished and ZrN pol and subgroup 8 with TiN pol, glass ZrN, glass TiN and glass Ti. There was a strong correlation between the number of FACs and the surface roughness (ANOVA; $P = 0.008$). The highest number of FACs was counted on surfaces with the lowest surface roughness: glass sheets coated with either Ti, TiN, or ZrN (R_a between 0.03 and 0.09 μm) and a TiN coating on polished Ti ($R_a = 0.06$ μm). Surfaces with an R_a between 0.23 and 2.2 μm (Ti 180, Ti 320 aligned, polymer coating, Ti GSP 2 and 8, Ti B 40 and Ti B 125) showed the lowest numbers of FACs.

The ratio FACs/CCSs (evaluated on a distance of 300 μm) showed similar results. There was again a strong correlation between the ratio FACs/CCSs and the surface roughness. The highest ratio FACs/CCSs was evaluated for fibroblasts cultured on surfaces with an R_a of 0.03 and 0.14 μm. The lowest values were determined for surfaces with an R_a between 0.23 and 2.2 μm (Ti 180, Ti 320 aligned, Ti GSP 2 and 8, Ti B 40 and 125, Ti 800 and Ti 1200). However, the Ti-coated glass surface ($R_a = 0.09$ μm) showed a significantly higher ratio compared with all other surfaces ($P < 0.001$). The means (FACs/CCSs) were divided into five homogeneous subgroups based on the Scheffé test (Fig. 3).

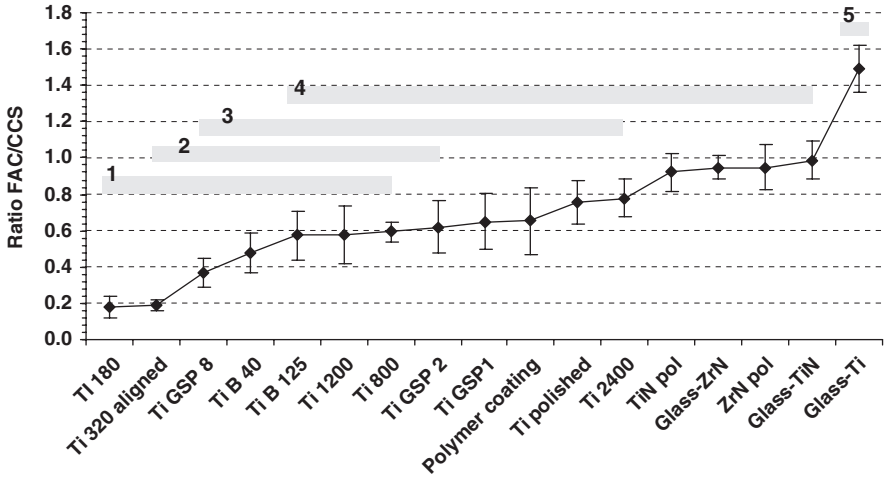

Fig. 3. Ratio of the number of focal adhesion contacts (FAC) to the number of cellular cross-sections (CCS) on a distance of 300 μm (transmission electron microscopy). The horizontal bars indicate homogeneous subgroups based on the Scheffé multiple comparison procedure.

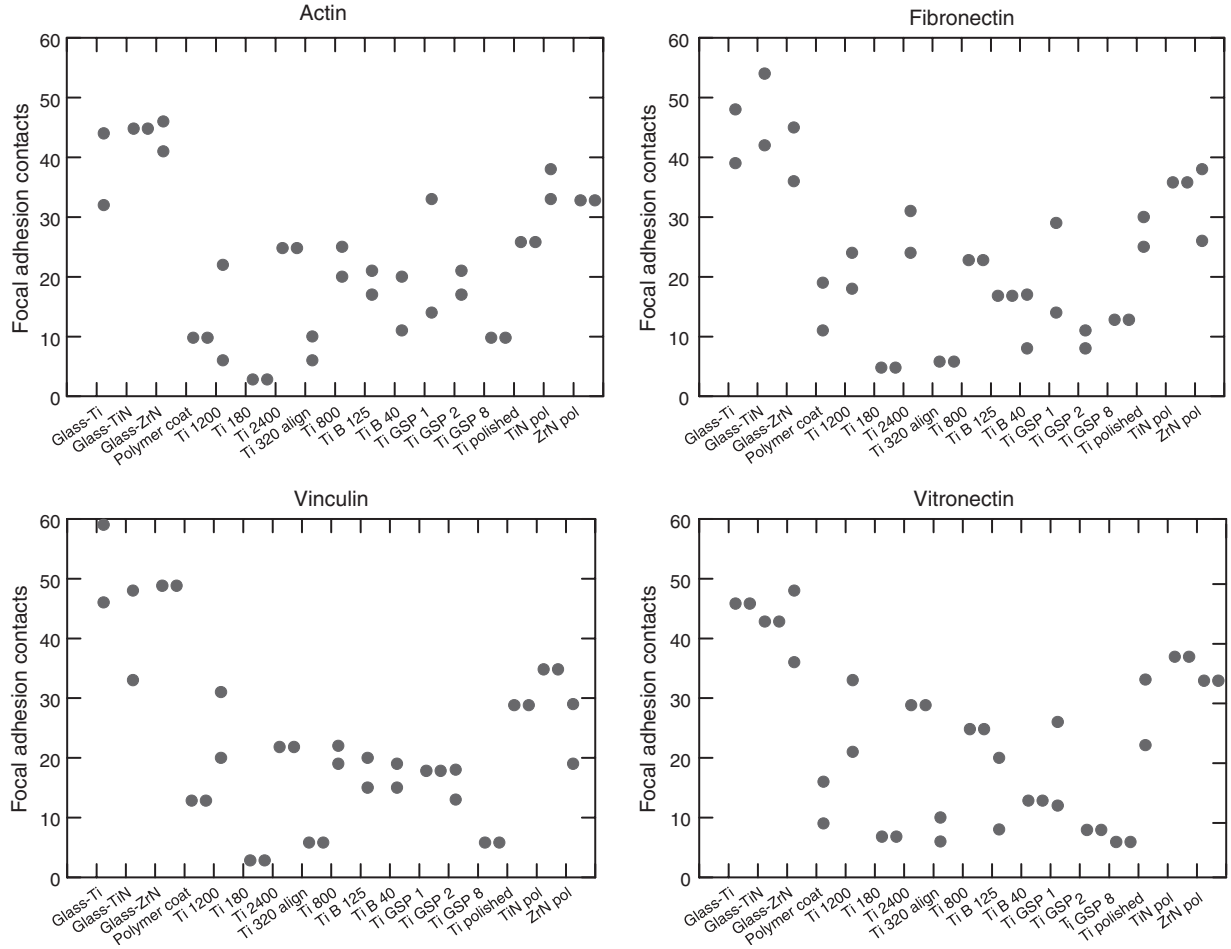

Fig. 4. Number of focal adhesion contacts containing adhesion molecules labeled with gold particles (10 nm, intracellular: actin and vinculin; extracellular: fibronectin and vitronectin) on a length of 300 μm (transmission electron microscopy). Every modified surface is represented by two dots ($n = 2$ samples), either one upon another (values were different from each other) or side by side (similar values).

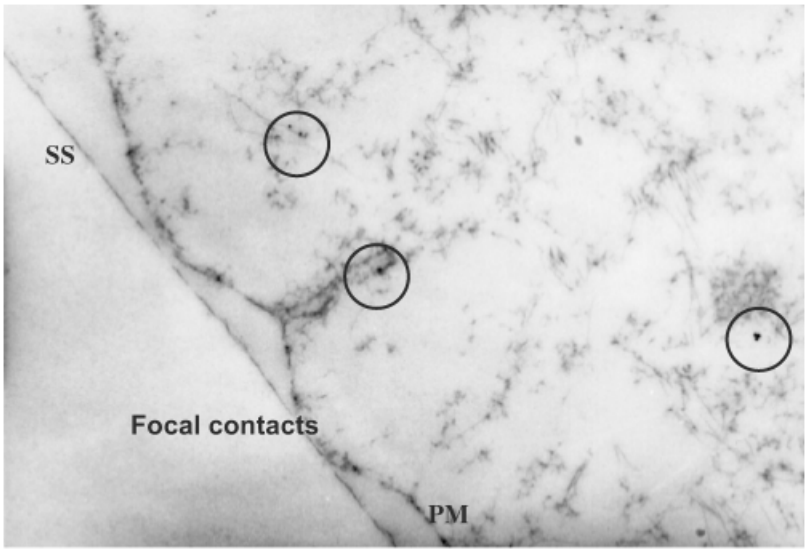

Fig. 5. Focal adhesion contact of a human gingival fibroblast growing on a TiN-coated glass surface (transmission electron microscopy). Circles: adhesion molecule (vinculin) labeled with gold particles (10 nm). PM, plasma membrane; SS, surface of the substratum (magnification: × 67000).

There were significant differences between two subgroups: subgroup 1 with Ti 180, Ti aligned, Ti GSP 8, Ti B 40, Ti B 125, Ti 1200, Ti 800 and subgroup 5 with glass Ti. The resulting values of the surfaces TiN pol, glass ZrN, ZrN pol and glass TiN were very similar within subgroup 4.

Immunogold labeling

Visualization of the extracellular fibronectin and vitronectin molecules and the intracellular actin and vinculin in FAC areas using the immunogold-labeling method showed distinct tendencies (Figs 4 and 5). The highest number of gold-conjugated actin in FACs was calculated for glass sheets coated with TiN, Ti and ZrN and Ti 800/1200/2400. FACs labeled with vinculin-conjugated gold particles were the highest on glass sheets coated with TiN, followed by Ti- and ZrN-coated glass, Ti GSP 1 and polished Ti. Immunogold labeling of ECM molecules revealed similar results. The highest number of gold conjugated fibronectin was determined on TiN-coated glass sheets, followed by a Ti and ZrN coating on glass and Ti 1200. The number of gold particles bound to vitronectin was distinctly higher in fibroblasts cultured on Ti-coated glass compared with glass sheets coated with ZrN or TiN, polished Ti, Ti 1200 and Ti GSP 1. The majority of the immunogold-labeled intra- and ECM molecules was detected on surfaces with the lowest surface roughness ($R_a = 0.03$–$0.52\ \mu m$). For both intracellular matrix molecules, glass sheets coated with TiN represented the highest number of gold particles. For vinculin and fibronectin as ECM molecules, the highest number of gold particles was counted on glass sheets coated with Ti.

Discussion

A major demand in designing oral implants is to produce a surface that promotes a strong attachment of the implant not only to bone but also to surrounding soft tissues. Hormia & Könönen (1994) demonstrated that surface processing influenced the adhesion of human gingival fibroblasts and the expression of adhesion-related molecules (focal contacts) on their membrane.

The primary goal of this investigation was to test the influence of different treatments of Ti or glass substrates as potential implant surfaces on FAC formation in human gingival fibroblast cultures. Therefore, 17 different modifications of glass or Ti substrates with the surface roughness varying between 0.03 and 2.2 μm were examined. Depending on the method of surface treatment, results of the spacing parameter measurements could be divided into three groups. Surfaces modified by PVD coating and polished Ti resulted in smooth surfaces with the lowest R_a and RS_m values, whereas the roughest surfaces showed the highest RS_m values. Within each group, surfaces with similar R_a values also showed similar values of the mean spacing of profile irregularities.

The number of FACs and the ratio FACs/CCSs determined at a length of 300 μm in ultrathin sections (TEM) revealed a strong correlation with the surface roughness of the substrate. No direct correlation was found with the spacing parameter.

The highest number of FACs was counted on surfaces with the lowest surface roughness ($R_a = 0.03$–$0.09\ \mu m$): glass sheets coated with either Ti, TiN, or ZrN. Additionally, the ratio FACs/CCSs was significantly higher on Ti-coated glass surfaces ($R_a = 0.09\ \mu m$) compared with all other surfaces. These results are similar to the results obtained in a study of Hormia & Könönen (1994). In their study, they examined the adhesion and spreading of human gingival fibroblasts on glass and differently processed Ti surfaces by immunolocalization of vinculin and the α- and β-subunits of the fibronectin and vitronectin receptors. Vinculin-containing focal contacts were present on surfaces with an R_a between $0.14 \pm 0.05\ \mu m$ (glass or electropolished Ti) and $0.41 \pm 0.14\ \mu m$ (etched Ti). Fibroblasts on rougher surfaces like sandblasted Ti ($R_a = 0.8 \pm 0.11\ \mu m$) lack focal contacts, which is not in accordance with our findings. Our study showed focal contacts on all surfaces examined but their number decreased with increasing surface roughness. In experiments performed by Dunn & Brown (1986), it was shown that the distribution of actin cables that are generally co-aligned with their associated focal contacts in fibroblasts could be influenced by the shape of the substratum. Actin cables extend obliquely into the cytoplasm from sites of adhesion and as proposed by Dunn (1991) could not become assembled in a bent state as it might be the case on rougher or structured surfaces. Fibroblasts do not always bridge grooves, but they can form focal adhesions to the side and bottom of even quite fine grooves (Brunette 1986; Dunn & Brown 1986; Clark et al. 1990, 1992; Meyle et al. 1993). On very smooth surfaces, as used in our experiments (e.g., Ti-glass, ZrN/TiN-glass, Ti-pol, Ti 2400), fibroblasts might be capable of optimizing the alignment of actin cables, and as observed by SEM,

were mainly spindle shaped and elongated with no clear orientation. Moreover, studies by Könönen et al. (1992) and Rahn et al. (1982) demonstrated that a smooth surface allow a more intimate contact between cells and the substrate than do rougher surfaces. Therefore, fibroblasts on smooth substrata may exhibit the comparatively highest number of focal adhesion sites as seen in our experiments.

The organic–inorganic nanocomposite polymer coating applied on polished Ti has been designed as a so-called easy-to-clean surface coating. Preliminary experiments indicate that intraoral biofilm formation on Ti specimens coated by this organic–inorganic nanocomposite is strongly reduced as compared with uncoated polished Ti. In the present study, the ratio FACs/CCSs on polymer-coated Ti specimens did not differ significantly as compared with polished Ti surfaces. Thus, the polymer coating might be an interesting approach to reduce bacterial adherence and simultaneously allowing fibroblast attachment.

In addition to surface topography, physicochemical properties of implant materials including mechanical rigidity and wettability (surface-free energy) may affect cellular behavior. The wettability of the surface plays an important role with respect to protein adsorption, cell attachment and spreading (Grinnell 1978; Baier et al. 1984; Schakenraad et al. 1986). Surfaces with a high surface-free energy (contact angle below 90°) are reported to be more adhesive than those with a low surface free energy (contact angle higher 90°). In contrast to these findings, den Braber et al. (1995) found that physicochemical parameters such as wettability and surface free energy play no measurable role in the shape and orientation of cells on microtextured surfaces. Contact angle measurements in our study showed distinct differences between surface modifications, revealing a strong dependence on surface morphology and mode of production. However, it should be kept in mind that the method for contact angle measurement used here shows the highest reproducibility on smooth surfaces. Therefore, results should be interpreted with caution and only surface modifications that show droplets that did not spread in all directions were included in our study. Glass substrates coated with ZrN or TiN with the lowest R_a (0.03 μm) showed the highest contact angle with 109.1°. PVD-coating of polished Ti did not change the contact angle; values for polished Ti and ZrN pol or TiN pol were comparable. The distinctly higher values for glass surfaces might be the result of a different sputtering process that might result in changes of the surface free energy by charging of the nonconductive glass surface. Rough surfaces (R_a between 0.52 and 2.2 μm; Ti GSP1, Ti GSP8, Ti B125) revealed the best wettability. The roughness enhances the wettability of the surface modifications under investigation from a hydrophobic (contact angle >90°) to a hydrophilic character (contact angle <90°). However, in clinical applications, the oral environment may alter surface free energies as shown by van Dijk et al. (1987). Salivary protein adsorption reduces differences originally present in surface free energies. Even though in our study glass surfaces showed the lowest wettability, the number of FACs and the ratio of FACs/CCSs were significantly higher than on rougher surfaces. Surface roughness seems to have a higher influence on FAC formation than surface wettability. Furthermore, as focal contacts represent the sites for the strongest cell-to-substrate adhesion, our results suggest that rougher surfaces (R_a between 0.2 and 2.2 μm) are less effective in supporting fibroblast adhesion.

Visualization of the extracellular fibronectin and vitronectin molecules and the intracellular actin and vinculin in FAC areas using the immunogold-labeling method showed distinct tendencies. However, because of the low sample size of two for each of the 17 surfaces only a descriptive analysis of the results was possible. For all of the four matrix molecules examined, the highest number of gold particles was counted on surfaces with the lowest roughness: glass sheets coated with Ti, TiN or ZrN. No distinct differences between these three hard coatings were observed. Polished Ti coated with TiN or ZrN followed next. These results suggest that all of the three hard coatings used either on glass or on polished Ti seem most suitable in supporting fibroblast adhesion.

A previously performed *in vitro* study revealed that the MTT activity and total protein in mouse fibroblasts were significantly increased in fibroblasts cultured on a TiN-coated polished Ti surface (R_a = 0.19 μm) compared with an uncoated polished Ti surface of a similar roughness (Grössner-Schreiber et al. 2003). It was assumed that these differences are in part a result of the composition or the chemical properties of the TiN coating. The TiN coating used in that study could have enhanced fibroblast adherence and growth by masking the more reactive underlying Ti oxide surface. Cells cultured in medium containing serum proteins do not directly adhere to the substratum surface, but to an adsorbed layer of serum components, which could form on TiN (Jansen et al. 1989). These attachment proteins contain sites with peptides promoting cell attachment that are recognized by receptors on the cell surface (mostly by integrins). Even changes in protein conformation through interaction with the TiN surface might be possible.

Other *in vitro* and *in vivo* studies conducted in our lab have shown that Ti implant surfaces coated with TiN or ZrN reduce bacterial colonization compared with other clinically used implant surfaces (Grössner-Schreiber et al. 2001, 2004). Rough Ti implant surfaces exposed to the oral cavity promote the adherence of oral bacteria (Yoshinari et al. 2000). Similar to the process of FAC formation, surface roughness has been suggested to be more important in plaque accumulation than surface free energy (Nakazato et al. 1989; Quirynen et al. 1990, 1993). Therefore, an implant surface ideal to resist bacterial colonization should be mainly smooth to allow the formation of an epithelial seal that prevents plaque accumulation.

Additionally, the surface softness of uncoated Ti facilitates surface roughening on abutments during oral hygiene measures (Fox et al. 1990; Speelman et al. 1992). However, due to the hardness of the coatings (Ti, TiN or ZrN coatings are nonabrasive), their use for implant abutments might prevent surface roughening during professional oral hygiene procedures as demonstrated by Mengel et al. (2004) for TiN-coated abutments of dental implants.

In conclusion, the findings of the present study revealed that all surface modifications examined allowed fibroblast attachment and growth. Provided that a high number of FACs reflects good adhesion of

fibroblasts *in vitro* smooth Ti surfaces with R_a values between 0.03 and 0.1 μm in combination with hard coatings may represent recommendable implant surfaces for clinical use. Moreover, the property of hard coatings to reduce bacterial adherence and to support fibroblast growth might reduce the possibility, or at least the severity, of peri-implantitis *in vivo*.

Acknowledgements: The authors wish to thank the FRIADENT GmbH (Mannheim, Germany) for providing the polished Ti discs. The present study was supported by the Deutsche Forschungsgemeinschaft (GR 963/2-1; GR 1421-2-1).

要旨

歯科インプラントの設計において主要な考慮点は、骨、結合組織および上皮が強力に付着するようなインプラント表面を創りだすことである。本研究は、チタン・インプラントの様々な表面処理が、局所の付着接触の形成に及ぼす影響を、線維芽細胞の培養において検討した。ヒト歯肉線維芽細胞を、物理蒸着法（ＰＶＤ）によってチタン（Ｔｉ）、窒化チタン（ＴｉＮ）、硝酸ジルコニウム（ＺｒＮ）を各々コーティングしたガラス板とチタン研磨ディスク、あるいは異なる表面性状を有するチタン・ディスク上で培養した。全ての修飾表面の特性指摘をするために、接触式スタイラス側面計を用いて表面粗さとスペーシングに関するパラメータを推計した。接触角度の測定に基づいて、表面エネルギーを計算した。線維芽細胞は、播種後３日目に透過電子顕微鏡（ＴＥＭ）で観察し、局所の付着接触率（ＦＡＣ）とＦＡＣ／細胞断面積の比率（CCSs）を、極薄切片において３００μｍの長さで測定した。細胞外の **fibronectin** と **vitronectin** 分子および局所付着接触領域の細胞内 **actin** と **vinculin** を視認するために、イムノゴールド標識を行った。結果は、**FAC**ｓの値と表面粗さの間の強い相関性を示した。粗さが最も少ない表面、すなわち **Ti**、**TiN** または **ZrN** をコーティングしたガラス板（**Ra**＝０．０３－０．１μ**m**）上で、最高数の **FAC** と大半のイムノゴールド標識された細胞内、外のマトリクス分子が認められた。これらの表面はヒト歯肉線維芽細胞の細胞付着に有利であると思われる。さらに過去の研究において、硬いコーティングは細菌付着を減少させることが示されている。

References

Baier, R.E., Meyer, A.E., Natiella, J.R., Natiella, R.R. & Carter, J.M. (1984) Surface properties determine bioadhesive outcomes: methods and results. *Journal of Biomedical Materials Research* **18**: *327–355*.

Bollen, C.M., Papaioanno, W., Van Eldere, J., Schepers, E., Quirynen, M. & van Steenberghe, D. (1996) The influence of abutment surface roughness on plaque accumulation and peri-implant mucositis. *Clinical Oral Implants Research* **7**: 201–211.

Brunette, D.M. (1986) Fibroblasts on micromachined substrata orient hierarchically to grooves of different dimensions. *Experimental Cell Research* **164**: 11–26.

Brunette, D.M. (1988) The effects of implant surface topography on the behavior of cells. *International Journal of Oral & Maxillofacial Implants* **3**: 231–246.

Burridge, K. & Chrzanowska-Wodnicka, M. (1996) Focal adhesions, contractility, and signaling. *Annual Review of Cell and Developmental Biology* **12**: 463–518.

Burridge, K. & Fath, K. (1989) Focal contacts: transmembrane links between the extracellular matrix and the cytoskeleton. *Bioessays* **10**: 104–108.

Burridge, K., Fath, K., Kelly, T., Nuckolls, G. & Turner, C. (1988) Focal adhesions: transmembrane junctions between the extracellular matrix and the cytoskeleton. *Annual Review of Cell Biology* **4**: 487–525.

Clark, P., Connolly, P., Curtis, A.S., Dow, J.A. & Wilkinson, C.D. (1990) Topographical control of cell behaviour: II. Multiple grooved substrata. *Development* **108**: 635–644.

Clark, P., Connolly, P. & Moores, G.R. (1992) Cell guidance by micropatterned adhesiveness in vitro. *Journal of Cell Science* **103**: 287–292.

Den Braber, E.T., de Ruijter, J.E., Smits, H.T., Ginsel, L.A., von Recum, A.F. & Jansen, J.A. (1995) Effect of parallel surface microgrooves and surface energy on cell growth. *Journal of Biomedical Materials Research* **29**: 511–518.

Dunn, G.A. (1991) How do cells respond to ultrafine surface contours? *Bioessays* **13**: 541–543.

Dunn, G.A. & Brown, A.F. (1986) Alignment of fibroblasts on grooved surfaces described by a simple geometric transformation. *Journal of Cell Science* **83**: 313–340.

Fox, S.C., Moriarty, I.D. & Kusy, R.P. (1990) The effects of scaling a titanium implant surface with metal and plastic instruments. An *in vitro* study. *Journal of Periodontology* **61**: 485–490.

Grinnell, F. (1978) Cellular adhesiveness and extracellular substrata. *International Review of Cytology* **53**: 65–144.

Grössner-Schreiber, B., Griepentrog, M., Haustein, I., Müller, W.-D., Lange, K.-P., Briedigkeit, H. & Göbel, U.B. (2001) Plaque formation on surface modified dental implants. *Clinical Oral Implants Research* **12**: 543–551.

Grössner-Schreiber, B., Hannig, M., Duck, A., Griepentrog, M. & Wenderoth, D.F. (2004) Do different implant surfaces exposed in the oral cavity of humans show different biofilm compositions and activities? *European Journal of Oral Sciences* **112**: 516–522.

Grössner-Schreiber, B., Neubert, A., Müller, W.-D., Hopp, M., Griepentrog, M. & Lange, K.-P. (2003) Fibroblast growth on surface modified dental implants. *Journal of Biomedical Materials Research* **64A**: 591–599.

Hormia, M. & Könönen, M. (1994) Immunolocalization of fibronectin and vitronectin receptors in human gingival fibroblasts spreading on titanium surfaces. *Journal of Periodontal Research* **29**: 146–152.

Hormia, M., Könönen, M., Kivilahti, J. & Virtanen, I. (1991) Immunolocalization of proteins specific for adhaerens junctions in human gingival epithelial cells grown on differently processed titanium surfaces. *Journal of Periodontal Research* **26**: 491–497.

Inoue, T., Cox, J.E., Pilliar, R.M. & Melcher, A.H. (1987) Effect of the surface geometry of smooth and porous-coated titanium alloy on the orientation of fibroblasts *in vitro*. *Journal of Biomedical Materials Research* **21**: 107–126.

Jansen, J.A., van der Waerden, J.P. & de Groot, K. (1989) Epithelial reaction to percutaneous implant materials: *in vitro* and *in vivo* experiments. *Journal of Investigative Surgery* **2**: 29–49.

Kilpadi, D.V. & Lemons, J.E. (1994) Surface energy characterization of unalloyed titanium implants. *Journal of Biomedical Materials Research* **28**: 1419–1425.

Könönen, M., Hormia, M., Kivilahti, J., Hautaniemi, J. & Thesleff, I. (1992) Effect of surface processing on the attachment, orientation, and proliferation of human gingival fibroblasts on titanium. *Journal of Biomedical Materials Research* **26**: 1325–1341.

Lodish, H., Baltimore, D., Berk, A., Zipursky, S., Matsudaira, P. & Darnell, J. (1995) *Molecular Cell Biology*. New York: Scientific American Books Inc.

Mengel, R., Meer, C. & Flores-de-Jacoby, L. (2004) The treatment of uncoated and titanium nitride-coated abutments with different instruments. *International Journal of Oral & Maxillofacial Implants* **19**: 232–238.

Meyle, J., Wolburg, H. & von Recum, A.F. (1993) Surface micromorphology and cellular interactions. *Journal of Biomaterials Applications* **7**: 362–374.

Milosev, I. & Navinsek, B. (1994) A corrosion study of TiN (physical vapour deposition) hard coatings deposited on various substrates. *Surface and Coatings Technology* **63**: 173–180.

Mustafa, K., Silva Lopez, B., Hultenby, K., Wennerberg, A. & Arvidson, K. (1998) Attachment and proliferation of human oral fibroblasts to titanium

surfaces blasted with TiO_2 particles. A scanning electron microscopic and histomorphometric analysis. *Clinical Oral Implants Research* **9**: 195–207.

Nakazato, G., Tsuchiya, H., Sato, M. & Yamauchi, M. (1989) *In vivo* plaque formation on implant materials. *International Journal of Oral & Maxillofacial Implants* **4**: 321–326.

Okumiya, M. & Griepentrog, M. (1999) Mechanical properties and tribological behavior of TiN–CrAlN and CrN–CrAlN multilayer coatings. *Surface and Coatings Technology* **112**: 123–128.

Pitaru, S., Gray, A., Aubin, J.E. & Melcher, A.H. (1984) The influence of the morphological and chemical nature of dental surfaces on the migration, attachment, and orientation of human gingival fibroblasts *in vitro*. *Journal of Periodontal Research* **19**: 408–418.

Quirynen, M., Bollen, C.M., Papaioannou, W., Van Eldere, J. & van Steenberghe, D. (1996) The influence of titanium abutment surface roughness on plaque accumulation and gingivitis: short-term observations. *International Journal of Oral & Maxillofacial Implants* **11**: 169–178.

Quirynen, M., Marechal, M., Busscher, H.J., Weerkamp, A.H., Darius, P.L. & van Steenberghe, D. (1990) The influence of surface free energy and surface roughness on early plaque formation. An in vivo study in man. *Journal of Clinical Periodontology* **17**: 138–144.

Quirynen, M., van der Mei, H.C., Bollen, C.M., Schotte, A., Marechal, M., Doornbusch, G.I., Naert, I., Busscher, H.J. & van Steenberghe, D. (1993) An *in vivo* study of the influence of the surface roughness of implants on the microbiology of supra- and subgingival plaque. *Journal of Dental Research* **72**: 1304–1309.

Rahn, B., Gerber, H. & Simpson, J. (1982) Cultured cells contacting implant material of different surface treatment. In: Winter, G.D., Gibbons, D.F. & Plenk, H., eds. *Advances of Biomaterials*, 39–44. New York: John Wiley.

Scarano, A., Piattelli, M., Caputi, S., Favero, G.A. & Piattelli, A. (2004) Bacterial adhesion on commercially pure titanium and zirconium oxide disks: an *in vivo* human study. *Journal of Periodontology* **75**: 292–296.

Scarano, A., Piattelli, M., Vrespa, G., Caputi, S. & Piattelli, A. (2003) Bacterial adhesion on titanium nitride-coated and uncoated implants: an *in vivo* human study. *Journal of Oral Implantology* **29**: 80–85.

Schakenraad, J.M., Busscher, H.J., Wildevuur, C.R. & Arends, J. (1986) The influence of substratum surface free energy on growth and spreading of human fibroblasts in the presence and absence of serum proteins. *Journal of Biomedical Materials Research* **20**: 773–784.

Schwarz, M.A., Owaribe, K., Kartenbeck, J. & Franke, W.W. (1990) Desmosomes and hemidesmosomes: constitutive molecular components. *Annual Review of Cell Biology* **6**: 461–491.

Speelman, J.A., Collaert, B. & Klinge, B. (1992) Evaluation of different methods to clean titanium abutments. A scanning electron microscopic study. *Clinical Oral Implants Research* **3**: 120–127.

Van Dijk, J., Herkstroter, F., Busscher, H., Weerkamp, A., Jansen, H. & Arends, J. (1987) Surface-free energy and bacterial adhesion. An *in vivo* study in beagle dogs. *Journal of Clinical Periodontology* **14**: 300–304.

Yoshinari, M., Oda, Y., Kato, T., Okuda, K. & Hirayama, A. (2000) Influence of surface modifications to titanium on oral bacterial adhesion *in vitro*. *Journal of Biomedical Materials Research* **52**: 388–394.